



Research article

Experimental characterizations of hybrid natural fiber-reinforced composite for wind turbine blades



Temesgen Abriham Miliket^{a,d}, Mesfin Belayneh Ageze^{b,*}, Muluken Temesgen Tigabu^{a,c}, Migbar Assefa Zeleke^{e,f}

^a Bahir Dar Energy Centre, Bahir Dar Institute of Technology, Bahir Dar University, Bahir Dar, Ethiopia

^b Centre of Renewable Energy, Addis Ababa Institute of Technology, Addis Ababa University, Addis Ababa, Ethiopia

^c Faculty of Mechanical and Industrial Engineering, Bahir Dar Institute of Technology, Bahir Dar University, Bahir Dar, Ethiopia

^d Department of Mechanical Engineering, Institute of Technology, Woldia University, Woldia, Ethiopia

^e Department of Mechanical Engineering, Institute of Technology, Hawassa University, Hawassa, Ethiopia

^f Department of Mechanical Engineering, University of Botswana, Gaborone, 0061, Botswana

ARTICLE INFO

Keywords:

ANOVA

Biodegradable

Natural fiber-reinforced composite material

Taguchi methods

Wind turbine blade materials

ABSTRACT

Performances of hybrid Natural Fiber-Reinforced Composites (NFRCs) from E-glass, Nacha (*Hibiscus macranthus* Hochst. Ex-A. Rich.), and Sisal (*Agave sisalana*) fibers are investigated for wind turbine blades applications. The process of composite manufacturing was getting started with harvesting and extracting the fibers from undesired constituents. To improve the interfacial interaction between fibers, it was further treated with 5% of NaOH and remnants removal. The experiment was performed based on the Taguchi method, specifically with L₁₆ orthogonal array. Four levels of a natural fiber weight ratio (i.e. 5%, 10%, 15 %, and 20%) were considered during the composite preparations process while the weight of glass fiber was maintained at 5% and 10%. The composites are manufactured using the hand lay-up method, and the test specimens are as per American Society for Testing and Materials (ASTM) standards. Then, tensile, compressive, and flexural tests were carried out using a universal testing machine (UTM). Analysis of variance (ANOVA) was employed to determine the factors which affect the experimental responses. Hence, in the main effect, it was confirmed that Nacha fiber (%wt of N) significantly contributes to tensile, compressive, and flexural strength at a 95% level of confidence. Furthermore, the optimal fiber compositions of composites are determined based on a higher signal-to-noise ratio (S/N) for the corresponding strengths.

1. Introduction

Blades are the most important and expensive part of a wind turbine component [1], which suffers diversified load conditions such as dynamic-wind force, cyclic load, gravitational forces, etc [2, 3]. Considering this and other factors international protocols like ASTM, ISO, and others are provided to meet the standard structural requirements of the wind turbine blade [4]. Attempts to show a high strength-to-weight ratio of materials must be considered during the structural development of the blades [5, 6]. However, the blade weight is further affected by various factors such as airfoils type [7], turbine geometry, material type, etc. Hence, proper choice of material with sophisticated manufacturing procedures is compulsory to provide stiffer blade surface quality [8]. This also helps to detach undesirable external

blade weight such as clay and snow suspended to a surface [9]. Therefore, multi-perspective considerations such as types of wind turbine, turbine capacity, blade material type, and blades manufacturing methods are crucial. Wind turbine blades are manufactured from either synthetic or natural fibers composites [10]. Now a day glass and carbon fibers are widely incorporated in mega-scale wind power generators, while aluminum alloy, aramid, and sometimes hybrid fibers reinforced composites are applicable for medium and small scale blade designs [1, 11, 12]. Generally speaking, modern turbine blade materials are expected to provide high energy yield, low weight, low cost, environmentally friendly, and extended durability.

Several studies show that every kW of wind power needs 10 kg of wind turbine (WT) blade materials (10 kg/kW or 10 t/MW), predicted that there will be nearly 50,000 tonnes of blade waste in 2020 and that

* Corresponding author.

E-mail addresses: elzmeal@yahoo.com, Mesfin.belayneh@aau.edu.et (M.B. Ageze).

this number exceeded 200,000 tonnes in 2034 [13] and it will reach 43 million tonnes by 2050 [14]. Furthermore, most recycling technologies are in the development stage and traditional end-of-life disposal methods allow significant environmental depletion [15, 16, 17]. Despite the recycling process, other factors such as economic aspects of material selection, material availability, raw material cost, and manufacturing costs must be considered for the practical viability of the turbine [12, 18]. For these reasons, over the last few decades attempts are being made on lingo-cellulose materials for next-generation structural applications [19], which are readily available in plants, animal products, or other minerals [20]. These materials are interestingly reliable and cost-effective especially for developing countries [21, 22], to capture on-site wind power by manufacturing the blades from local composite materials [23, 24]. The important characteristics of natural fibers include good mechanical properties, no-environmental impacts, non-corrosive, biologically degradable, cost-effectiveness, etc [25].

Some attempts show NRFCs are applicable for WT blade applications. For example, green materials such as brich, spruce bamboo, and Douglas fir were being approved for large-scale HAWT in the US [26, 27, 28]. Holmes et al. [29] suggested the attractiveness of bamboo-based composite for wind turbine blade material applications. Shah et al. [30] further confirmed the suitability of flax reinforced composite for wind turbine blade applications. Therefore, to enhance the structure of the wind turbine blade, the mechanical properties should be improved by hybridization [31, 32, 33]. This can be done by combining two or more distinct materials together with surrounding matrix and creating enhanced properties [34]. Alene & Tilahun [35] studied bamboo/E-glass hybrid composite and approved at an equal fiber weight ratio (50:50) can have sufficient potential to be used for wind turbine blade shell design.

However, due to their hydrophilic nature and low thermal stability of the raw fiber, mechanical behavior could be affected by the humidity [3]. This mainly affects the micro and/or macrostructure of the composite. Hence, fiber hybridization becomes more fundamental for the better structural performance of composites. The main aim of this paper is to investigate the mechanical characteristics of hybrid composite material prepared from Nacha and Sisal plant fibers, as demonstrated in Figure 1. The properties of Nacha or *Hibiscus macranthus* Hochst. ex A. Rich. which is categorized in Malvaceae family [36], and Sisal (*Agave sisalana*) are investigated for wind turbine blade application. Nacha is the local name of the plant and due to its high strength, its fiber is traditionally used to make rope and baskets [37]. Polyester and hardener are taken as matrix and binder for the composites. This study intends to study the mechanical properties of hybrid composite material for wind turbine blade applications. This may be good practice by contributing low-cost and locally available conventional materials for sustainable power generation applications. Furthermore, this paper present the mechanical

properties of a hybrid composite material made from Nacha and Sisal plant fibers experimentally as an alternative material for wind turbine blades.

This paper is organized into four main sections: the background of the study is followed by a brief framework of experiment design and methods. Finally, the results are presented with statistical analysis followed by discussions, and remarks for future development.

2. Materials and methods

2.1. Materials

The current research is focused on the mechanical properties of a reinforced composite made from Ethiopia's two most common plant fibers. Sisal leaves and Nacha stem are collected from the Abay (Blue Nile) river basin around Bahir-Dar city, Ethiopia. Then, commercially available glass fiber and unsaturated polyester resins have been used because of their short cure time and low cost [38].

2.2. Methods

The experiment encompasses, fiber extraction, composite preparation, and characterization of the samples for tensile, compressive, and flexural strength, as shown in Figure 2.

Fiber Extraction: Sisal leaves and Nacha stems are collected from the plant's origin manually. To easily extract the fibers from its constituents, the leaves and stems were retted into river water for 28 and 21 days, respectively, until a pure individual fiber was identified. This technique was adopted to remove unwanted constituents from the fiber by allowing microbial degradation in the water [39]. Then, it was dried with sunlight at atmospheric conditions to remove the moisture from the fiber [40]. This extraction process is very simple, easy, cheap, and provides good quality of fiber [41, 42]. This technique is a very common and indigenous method in the rural areas of Ethiopia for fiber extraction for their day-to-day application. To ensure the quality of fibers within acceptable limits of mechanical properties, unwanted constituents such as hemicellulose, lignin, and wax must be removed. Hence, chemical treatment is allowed to improve the interfacial interaction between fiber and matrix [43]. However, the types of treatment methods significantly affect the mechanical property of the extracted fibers. Studies show NaOH is the most widely used chemical treatment for fiber surface modification to remove lingo-cellulosic components of the fiber [44, 45]. Under fiber to matrix weight ratio 30%wt sisal fiber 5% wt of NaOH exhibited maximum improvement in the tensile, flexural, and compressive strength [46]. However, when the alkali concentration is increased the fiber mechanical properties significantly worsened [47]. Hence, for this study, 5% of NaOH was undertaken during the treatment process of the fibers.



Figure 1. Plants were used for the study, (a) Nacha (b) Sisal.

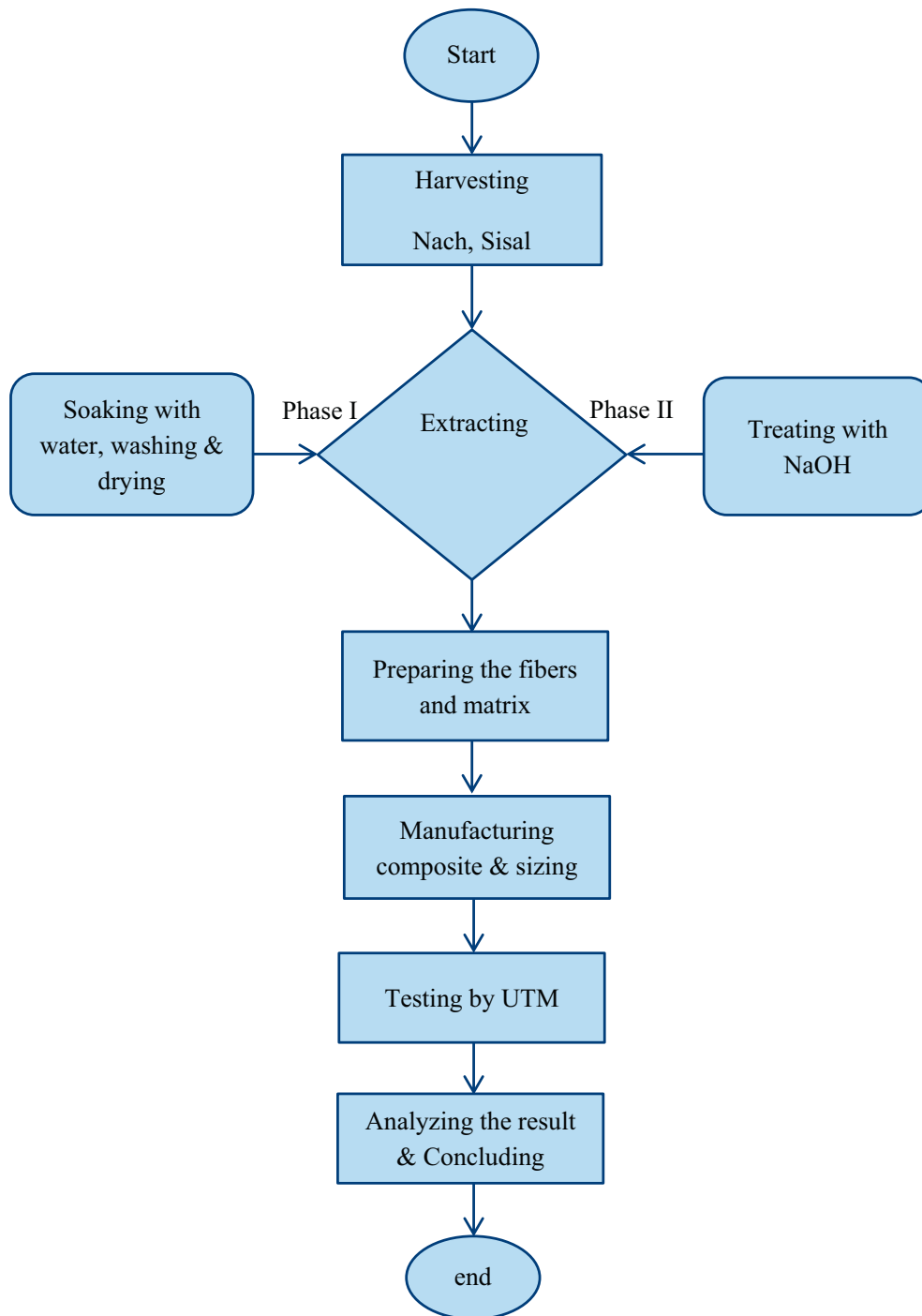


Figure 2. Working methodology.

Physical properties of the fiber: In composite production, the weight and volume fractions are determined from the fiber density, Table 1. Mathematically it can be calculated as, Eq. (1);

$$\rho_f = \frac{M_f}{L_f \left(\frac{\pi D_f^2}{4} \right)} \quad (1)$$

where: ρ_f , M_f , L_f , and D_f are the density, mass, length, and diameter of the fiber.

Whereas the strength is dependent on the diameter of a single fiber and it is measured by microphotographs with micrometers (μm). However, the diameter of the fibers varies greatly because of their irregular cross-

sectional shape. The second important physical property to be considered in natural fiber production is moisture absorption. It is measured with a pycnometer using the Archimedes principle, where the volume of fiber immersed in a liquid is equal to the volume of spilled liquid, Eq. (2).

Table 1. Physical and mechanical properties of individual fibers.

Material	Density (g/cm ³)	Moisture content (%)	Elongation at Break (%)	Ref.
Nacha fiber	1.38–1.43	7.8–12.46	1.4	[37, 48]
Sisal fiber	1.2	5–6	8	[49, 50]
Glass fiber	2.5	-	0.5	[51]



a) Fiber mat
 b) Ply arrangement
 c) Compression assisted hand layup mold
 d) Composites
 e) Cutting composite using hacksaw

Figure 3. Composite manufacturing process.

$$\rho_f = \frac{(m_2 - m_1)\rho_l}{(m_3 - m_1) - (m_4 - m_2)} \quad (2)$$

where:

- ρ_f and ρ_l are the density of the fiber and the liquid water in the pycnometer, respectively.
- $m_1, m_2, m_3,$ and m_4 are the mass of the pycnometer alone, filled with fiber, filled with liquid, and filled with fiber and liquid, respectively.

Composite Preparation: WT blades are subjected to diversified loading conditions [2, 3]. So the blade designers must identify proper fiber orientation that effectively withstands loading conditions and prolong its service life. The ratio might be able to be expressed by weight or by volume fraction of the components, but the fiber volume ratio can be derived from the fiber/matrix weight ratio. For better composite strength, the recommended fiber/matrix ratio (30%/70%) [52, 53], was used during the composite preparation.

The spacemen preparation of composite structures starts with the incorporation of several fibers into a thin layer of reinforcement matrix to form ply (lamina). The arrangement of fiber laminates is considering the major aerodynamic load along the wind turbine blades' span. Due to this fact, the mixed type fiber orientation (i.e. $0^\circ/90^\circ$ and $45^\circ/ - 45^\circ$) presented in [54] was considered for five-layered composite laminates of hybrid composite.

The compression-assisted hand lay-up technique demonstrated in Figure 3 (c), was used to increase the accuracy of fiber/matrix stacking and reduce the voids inside the composite. Sheet boxes of size $300 \times 25 \times 2$ mm were used for the molding process of tensile and flexural specimens. For the compatibility of the compressive setup, the thickness of the sheet box is slightly larger (i.e. $300 \times 25 \times 3$ mm). Then the mixture of resin and hardener was poured into the box and thoroughly filled. The composites were pressed with the slab and 6.7×10^2 Pa pressure was applied for 2 h to have the desired shape to minimize the void

formations. After curing, the mold was opened and separated from the slab, the surface was cleaned. Finally, the samples are manually cut and whipped out using glass paper until the desired ASTM standards are satisfied presented in Table 2.

2.2.1. Experimental design

To investigate the effect of composite %wt on mechanical properties values statistical data analysis was used based on the Taguchi method with signal to noise (S/N) ratio and ANOVA methods. These are the common statistical approaches for the predictions of optimum design results and to calculate the percentage contributions of possible responses such as tensile, flexural, and compressive strength respectively. Table 3 demonstrate control parameters (input factors) during composite fabrications and their levels. To ensure maximized S/N (η) ratio, Larger-the-better Taguchi principles have been used, Eqs. (3), (4), (5), and (6).

$$\eta = -10 \log \left(\frac{1}{n} \sum_{i=1}^n \frac{1}{y_i^2} \right) \quad (3)$$

where: n is the number of replication, y_i is the observed response value, and $i = 1, 2, \dots, n$

$$PC = \frac{SS_i}{SS_t} \times 100 \quad (4)$$

$$SS_i = \sum_{j=1}^l (SNR_{ij} - SNR_m)^2 \quad (5)$$

$$SS_t = \sum_{i=1}^n (SNR_i - SNR_m)^2 \quad (6)$$

where: PC is percentage contributions, SS_i is the sum of the square in i^{th} parameter, SS_t is the total sum of the square, SNR_{ij} is the signal-to-noise

Table 2. Specimen preparation standard.

Test type	Specimen Standard	Dimensions (mm)
Tensile	ASTM D 3039 [55]	$165 \times 19 \times 2$
Flexural strength	ASTM D 790 [56]	$126 \times 12.5 \times 2$
Compressive	ASTM D 3410 [57,58]	$37.5 \times 16.5 \times 3$

Table 3. Levels of control factors used in the experiment.

Levels	%wt of G	% wt of N	% of S
1	5	5	5
2	10	10	10
3	10	15	15
4	10	20	20

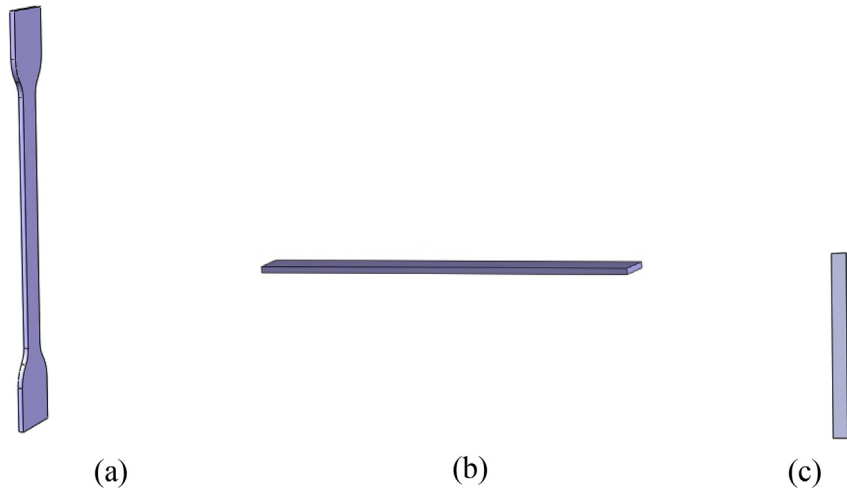


Figure 4. ASTM standard composites specimens (a) tensile; (b) flexural; (c) compressive.

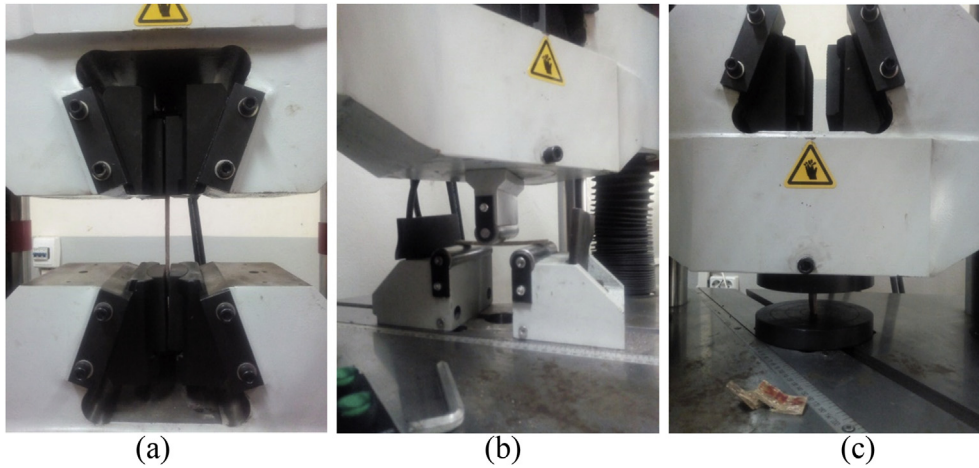


Figure 5. Experimental setups (a) Tensile; (b) Flexural; (c) Compressive.

Table 4. Experimental results of tensile strength with a corresponding S/N ratio.

Experiments	%wt of G	%wt of N	%wt of S	Tensile load (kN)	Tensile stress (MPa)	S/N
1	1	1	1	9.4	167.857	22.45926
2	1	2	2	11.82	207.22	24.44905
3	1	3	3	10.16	181.429	23.13458
4	1	4	4	11.2	200	23.98106
5	2	1	2	10.78	192.5	23.64908
6	2	2	1	11	196.429	23.82456
7	2	3	4	10.26	183.214	23.21965
8	2	4	3	9.76	174.286	22.7857
9	3	1	3	10.86	193.929	23.7133
10	3	2	4	12.58	220.12	24.99031
11	3	3	1	10.26	183.214	23.21965
12	3	4	2	12.34	216.26	24.823
13	4	1	4	10.24	182.857	23.2027
14	4	2	3	11.54	206.071	24.24082
15	4	3	2	11.22	195.44	23.99656
16	4	4	1	11.38	203.214	24.11955

Table 5. Experimental results of flexural strength with a corresponding S/N ratio.

Experiments	%wt of G	%wt of N	%wt of S	Flexural load (kN)	Flexural stress (MPa)	S/N
1	1	1	1	12.16	217.143	24.69537
2	1	2	2	11.82	211.071	24.44905
3	1	3	3	11.76	210	24.40485
4	1	4	4	9.88	176.429	22.89184
5	2	1	2	12.24	205.87	24.72271
6	2	2	1	10.76	107.6	23.60333
7	2	3	4	11.32	113.2	24.04401
8	2	4	3	11.78	117.8	24.38999
9	3	1	3	12.48	210.43	24.89138
10	3	2	4	11.14	111.4	23.90479
11	3	3	1	11.5	115	24.18104
12	3	4	2	12.1	201.19	24.62279
13	4	1	4	12.02	192.70	24.59479
14	4	2	3	11.86	211.786	24.4784
15	4	3	2	11.94	213.214	24.53679
16	4	4	1	9.56	195.6	22.57624

Table 6. Experimental results of compressive strength with a corresponding S/N ratio.

Experiments	% wt of G	% wt of N	% wt of S	Compressive load (kN)	Compressive stress (MPa)	S/N
1	1	1	1	12.04	267.556	24.61404
2	1	2	2	14.16	308.55	26.02278
3	1	3	3	12.74	283.111	25.1049
4	1	4	4	12.48	277.333	24.92581
5	2	1	2	11.72	260.444	24.38007
6	2	2	1	12.8	290.444	25.14607
7	2	3	4	12.52	278.222	24.9536
8	2	4	3	12	266.667	24.58514
9	3	1	3	10.36	230.222	23.30871
10	3	2	4	13.52	300.444	25.62105
11	3	3	1	13.9	291.37	25.86181
12	3	4	2	10.54	255.5	23.45973
13	4	1	4	10.86	289.47	23.72076
14	4	2	3	13.84	241.333	25.81876
15	4	3	2	13.74	307.556	25.76138
16	4	4	1	10.86	235.00	23.72141

ratio of i^{th} parameter at j^{th} level, SNR_m is the mean signal-to-noise ratio, l is the number of level and n is the number of experiment.

2.2.2. Mechanical tests

The specimens for mechanical tests (Figure 4) are prepared as per the ASTM standard specified in Table 2. The dimensions of samples of the composite were cut into the required shape using a hack saw and polished by glass paper. To increase the accuracy of the test result sixteen sets of experiments were tested with five replications. The experiment was conducted using UTM in the BiT available in the laboratory, shown in Figure 5. The manufacturer specifications of the UTM include; model WAW-600D, maximum load capacity 500kN, and the load accuracy below ±1%. The crosshead speed of the machine was maintained at 2 mm/mm under quasi-static conditions and constant temperature. During the test, the load was continuously applied for all specimens from the load cell until the specimen fails.

3. Results and discussion

The totals of five sample replications tests have been carried out to increase the adequacy of the experimental results and then the average of the tests are taken to decide the characteristics of the composite.

Table 7. ANOVA for S/N ratios for tensile strength.

Source	DF	Seq SS	Adj SS	Adj MS	F	P
%wt of G	3	1.6549	1.6549	0.5516	3.52	0.089
%wt of N	3	3.1787	3.1787	1.0596	6.75	0.024
%wt of S	3	1.7466	1.7466	0.5822	3.71	0.081
Residual Error	6	0.9414	0.9414	0.1569		
Total	15	7.5216				

Table 8. ANOVA for S/N ratios flexural strength.

Source	DF	Seq SS	Adj SS	Adj MS	F	P
%wt of G	3	0.284	0.284	0.09465	0.41	0.755
%wt of N	3	2.5156	2.5156	0.83852	3.59	0.086
%wt of S	3	2.2749	2.2749	0.75829	3.25	0.102
Residual Error	6	1.4008	1.4008	0.23346		
Total	15	6.4752				

Table 9. ANOVA for S/N ratios for compressive strength.

Source	DF	Seq SS	Adj SS	Adj MS	F	P
%wt of G	3	0.7732	0.77323	0.25774	0.57	0.656
%wt of N	3	8.5366	8.53661	2.84554	6.28	0.028
%wt of S	3	0.0841	0.0841	0.02803	0.06	0.978
Residual Error	6	2.7199	2.71991	0.45332		
Total	15	12.1139				

Table 10. Response table for S/N ratios for tensile strength.

Larger is better			
Level	%wt of G	%wt of N	%wt of S
1	23.51	23.26	23.41
2	23.37	24.38	24.23
3	24.19	23.39	23.47
4	23.89	23.93	23.85
Delta	0.82	1.12	0.82
Rank	3	1	2

Therefore the observation from a variety of recorded test results among the specimens in each of the three fiber weight ratios is discussed in the following few sections. Tables 4, 5, and 6 illustrate the response of DOE using the Taguchi method for tensile, flexural, and compressive strength of composites respectively. Experimental results with the corresponding S/N ratio are also presented in Tables 4, 5, and 6 respectively.

3.1. ANOVA test for S/N ratio

ANOVA is the statistical method of quantifying the values of errors that correspond to the differences in expected and predicted values of the responses. The error may be due to the presence of some uncontrollable conditions such as human error and environmental uncertainty during the experimentations. Therefore, to take into account these errors for which the significance level are assumed to be 5% (level of confidence to be 95%). When a P-value less than 5% indicates that more than 95% of the response are significantly caused by the factors and a model is a candidate for further exploration. Tables 7, 8, and 9 illustrates the ANOVA test result for tensile, flexural, and compressive strength of

Table 11. Response table for S/N ratios for flexural strength.

Larger is better			
Level	%wt of G	%wt of N	%wt of S
1	24.11	24.73	23.76
2	24.19	24.11	24.58
3	24.4	24.29	24.54
4	24.05	23.62	23.86
Delta	0.35	1.11	0.82
Rank	3	1	2

Table 12. Response table for S/N ratios compressive strength.

Larger is better			
Level	%wt of G	%wt of N	%wt of S
1	25.17	24.01	24.84
2	24.77	25.65	24.91
3	24.56	25.42	24.7
4	24.76	24.17	24.81
Delta	0.6	1.65	0.2
Rank	2	1	3

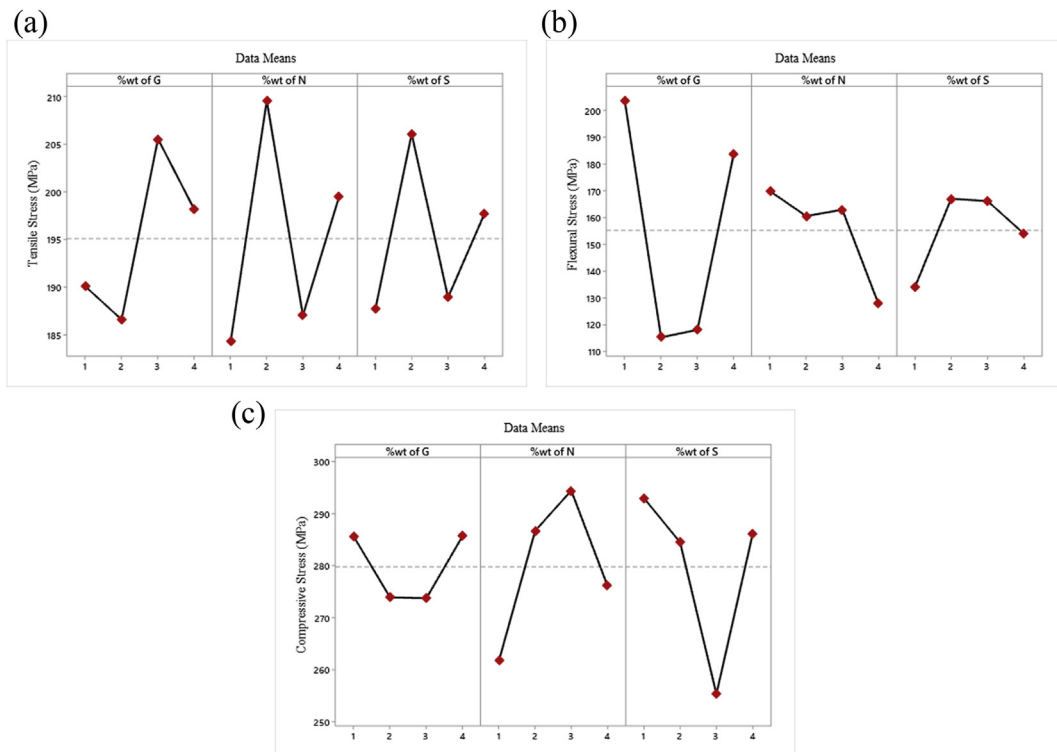


Figure 6. The main effect plots (a) tensile; (b) flexural; (c) compressive.

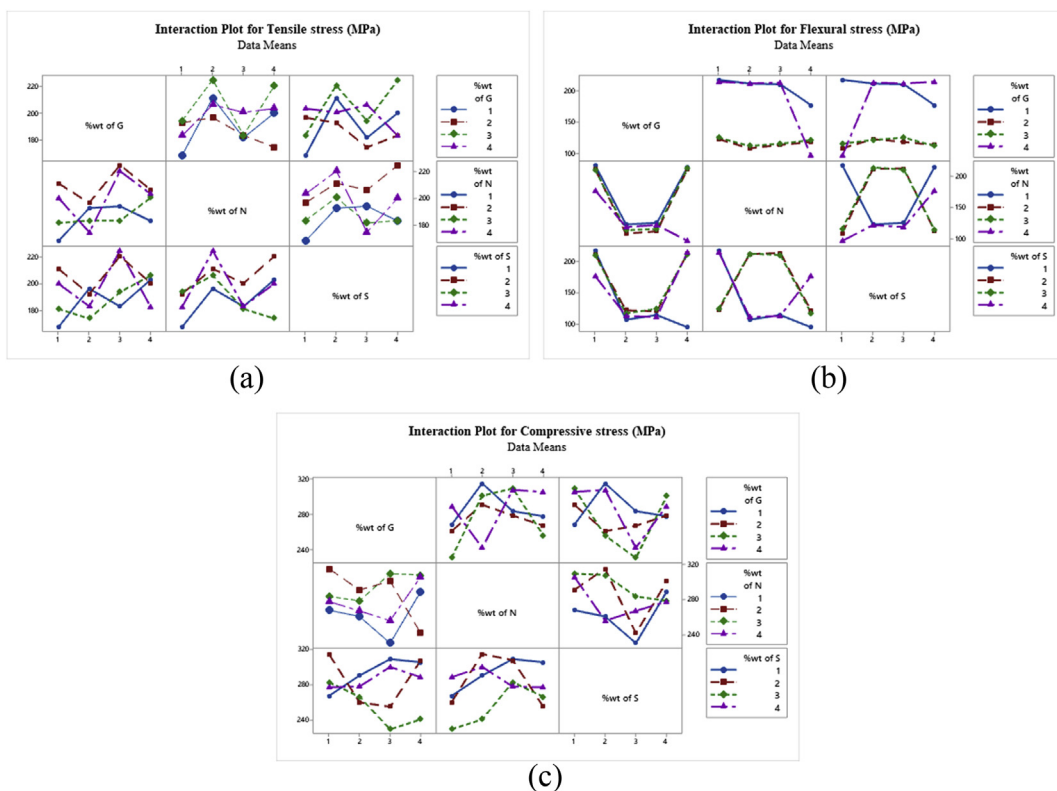


Figure 7. Interaction plots (a) tensile; (b) flexural; (c) compressive.

composites respectively. Hence, in these cases %wt of N achieves the requirements (P-value less than 5%) and it shows a significant contribution to all mechanical properties except flexural strength. Table 8 shows the P-value is greater than the reference value in which the factors

(i.e. %wt G, %wt N, and %wt S) did not show significant contributions on flexural strength. But the %wt of N fiber is in the primary rank among the factors. This involves further predictions (mathematical models) which are described in section 3.5 for optimal design. Furthermore, in this study

Table 13. Fiber composition (%wt) in four prior composites.

Test Type	Experiments	Fiber composition (%wt) in a composite					Rank
		G	N	S	σ_{max}	S/N	
Tensile	10	10	10	20	220.12	24.99031	I
	12	10	20	10	216.26	24.82304	II
	2	5	10	10	207.22	24.44905	III
	15	5	15	10	195.44	23.99656	IV
Flexural	9	10	5	15	210.43	24.89138	I
	5	10	5	10	205.87	24.72271	II
	12	10	20	10	201.19	24.62279	III
	13	10	5	20	192.70	24.59479	IV
Compression	2	5	10	10	308.55	26.02278	I
	11	10	15	5	291.37	25.86181	II
	13	10	10	15	289.47	25.81876	III
	15	10	15	10	235.00	25.76138	IV

neither %wt S nor %wt G shows significant contributions alone. Despite that, the fibers perform a better strength in the synergetic effects of hybrid composites which are illustrated in section 3.3.

3.2. Main effect

The effects of each control factor (%wt G, % wt N, and % wt S) on the response are obtained from the mean response table of the S/N ratio and the results are listed in Tables 10, 11, and 12. The main effect plot for the

S/N ratio of the corresponding mechanical properties is illustrated in Figure 6. It can be shown that the larger values of the S/N ratio represent the better quality of the material based on Taguchi DOE.

3.3. Interaction effects

All input factors under this study have a synergetic effect on the composite material. This section confirms which combination of the factors provides a better composite material. Figure 7 (a to c), shows the

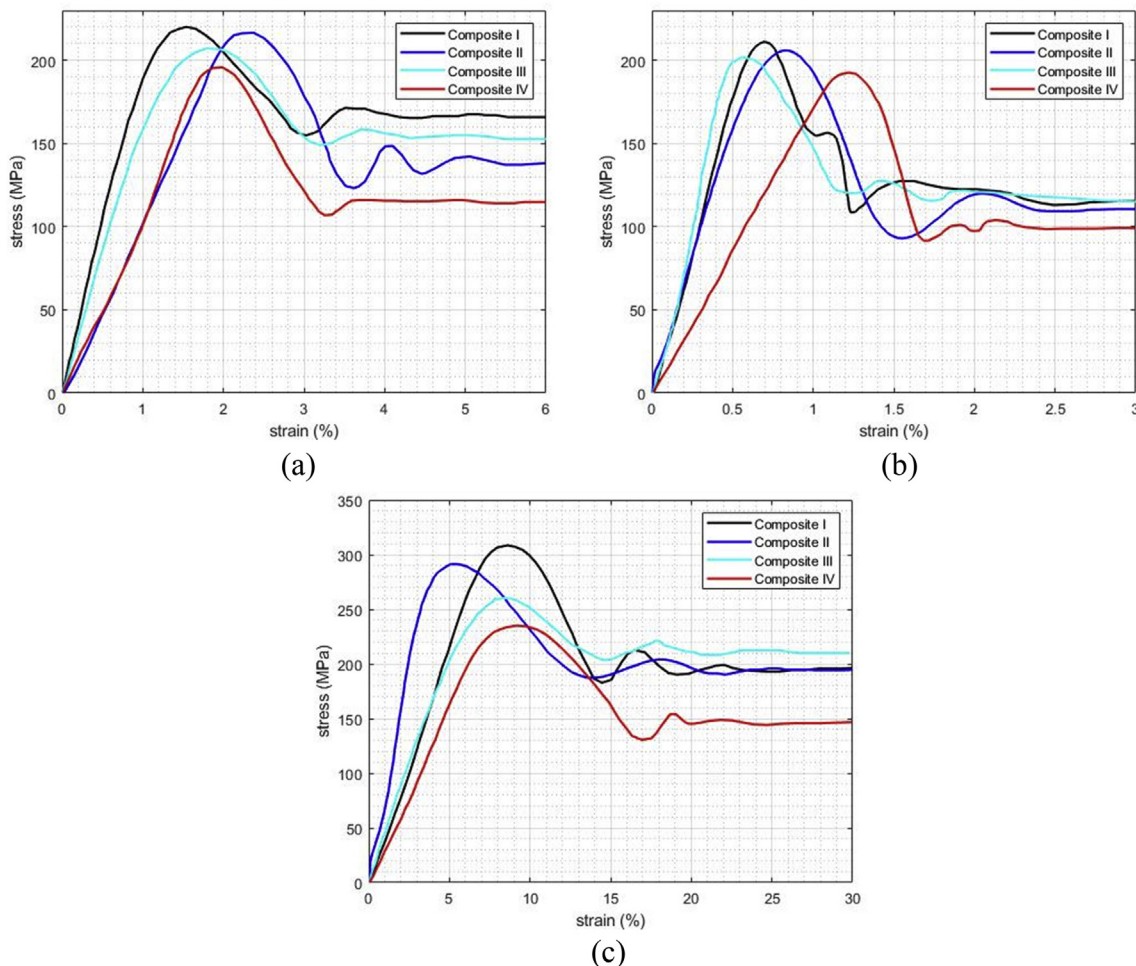


Figure 8. Stress-strain curves (a) tensile; (b) flexural; (c) compressive.

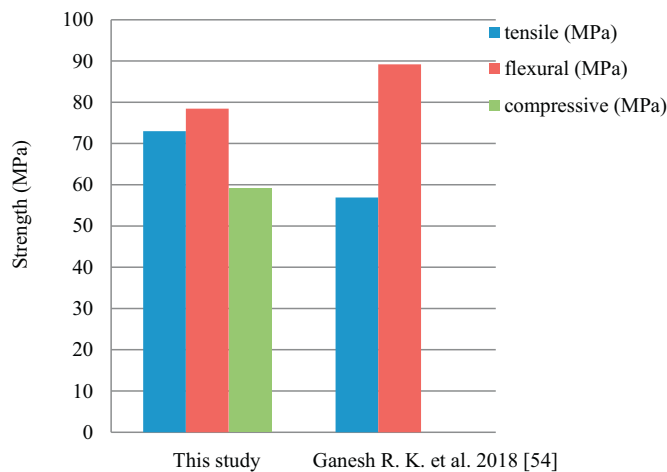


Figure 9. Result comparison with [54].

interaction effects of factors on the tensile, flexural, and compressive strength of the composite. The levels of the factors are indicated on the horizontal axis and collared legends, whereas their corresponding values are indicated on the vertical axis. In this interaction plot, the lines are not parallel and the more nonparallel indicates the greater the strength of the interaction of the factors. This interaction effect indicates that the composite strength is more likely depends on the nature of the fiber. For example, if we consider the upper half row of Figure 7 (a), the highest interaction between %wt of G and %wt of N, %wt of G and %wt of S and %wt of N and %wt of S are associated with the highest strength.

However, if we use the corresponding levels 4, 3, and 3, the values are associated with the mean strength. Despite when we observe Figure 7 (b), the factors at level 2 and 3 have linear relationships which indicate the interaction effects of the factors is very weak.

3.4. Stress-strain analysis

The stress-strain curves of the four prior composites are selected among sixteen experiments that show the better mechanical strengths under this investigation. According to our experiment, S/N is the important screening parameter used to identify control factors that reduce variability in production by minimizing the effects of uncontrollable factors (noise factors) which cannot be controlled during production but can be controlled during experimentation. In our DOE, a Taguchi-design of the experiment, identify optimal control factor settings that make the product robust, or resistant to variation from the noise factors. Hence, higher values of the S/N identify control factor settings that minimize the effects of the noise factors. Table 13 shows the summary of composites selected with a fiber composition and ranked based on S/N ratios. Among Taguchi L₁₆ array mentioned in Tables 5, 6, and 7, the corresponding experiments 10, 9, and 2 revealed the highest tensile, flexural, and compressive strengths respectively. Despite in most experiments the observations are affected by the mat sequence rather than the fiber weight ratio. During the plots the curves fitting was performed using MathLab, few outlier values are suppressed and create a normal distribution of more effective variables, see Figure 8.

Because poor interfacial interaction between the fibers and the matrices creates micro-cracks that will not propagate at relatively low loads and the microstructure can be stationary. The gradual increase in load results in a variety of internal stiffness and stress with a progressive microcrack growth and breakout [59]. This means that composite materials are extremely sensitive to failure by interlaminar through the application of concentrated loads [60].

The present work is compared with previously published hybrid NFRC (sisal, flax, and E-glass) works for the same application. Since no published works are available for hybrid Nacha composite hence we compare the current study with related works demonstrated in [54] for a similar purpose. For comparison, the strengths (tensile, compressive, and flexural) are determined for both studies. Figure 9 demonstrates the

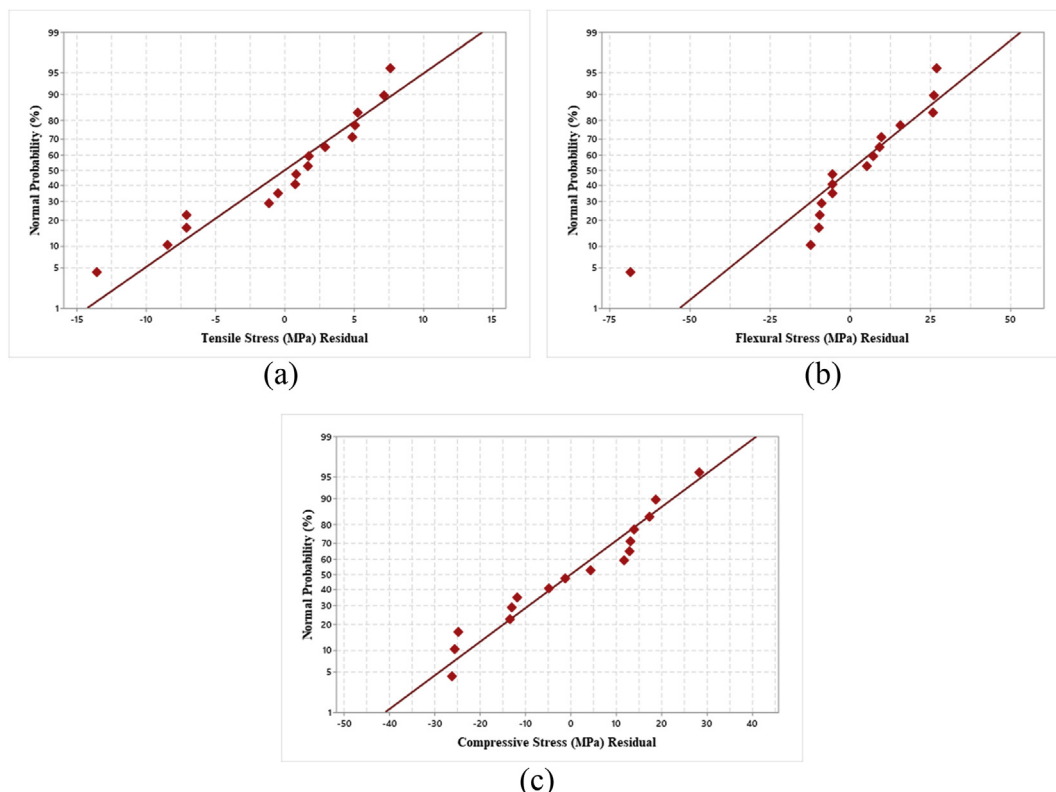


Figure 10. Normal probability plot (a) tensile; (b) flexural; (c) compressive.

comparison of the present work with related published work in [54] and the results are agreed well. Small deviations have occurred due to the characteristics of fiber (nacha instead of flax) and matrix (Polyester instead of Epoxy) affecting the composite strength.

3.5. Regression analysis

The linear regression mathematical model has been developed to predict the optimal relationship between factors and response, Figure 10. The predicted value of tensile, compressive, and flexural strength was calculated from Eqs. (7), (8), and (9). The error percentages between the predicted and measured values from each run of the experiments are calculated from Eq. (10).

$$\sigma_{t_optimal} = 175.4 + 4.30 \%wt \text{ of } G + 2.30 \%wt \text{ of } N + 1.29 \%wt \text{ of } S \text{ (MPa)} \quad (7)$$

$$\sigma_{f_optimal} = 173.0 + 1.8 \%wt \text{ of } G - 4.9 \%wt \text{ of } N - 1.6 \%wt \text{ of } S \text{ (MPa)} \quad (8)$$

$$\sigma_{c_optimal} = 279.4 + 0.02 \%wt \text{ of } G + 5.10 \%wt \text{ of } N - 4.97 \%wt \text{ of } S \text{ (MPa)} \quad (9)$$

$$\% \text{ error} = \left(\left(\frac{\text{Estimated value} - \text{Actual value}}{\text{Actual Value}} \right) \times 100 \right) \quad (10)$$

The average errors for tensile, flexural, and compressive strengths are -0.18%, 2.17%, and -0.49% respectively. The percentages of errors between experimental and predicted values are very low. This shows that the predicted value and measured value are closer and it can be concluded that the developed mathematical models are suitable and which is safe for optimal fiber synergetic composite strengths.

4. Conclusion

The core purpose of employing NFRCS materials for wind turbine structural application is a generation of energy without polluting the environment. Most modern wind turbines are designed from expensive synthetic materials for the average estimated life of 20–25 years, and after finishing the service life the components are traditionally disposed to the environment. Recent practices are attempting to replace synthetic materials with biodegradable fiber-based materials for next-generation wind turbine structural applications. But the process of enabling natural fiber for wind turbine blade design is a big challenge because the strength-to-weight ratio of the material must be high enough, and the structure expected to achieves at least proportional structural performance to that of synthetic once. To acquire these composite development processes including fiber type, fiber surface modification, treatment type, composite manufacturing method, enhanced moisture absorption reduction techniques, etc plays a vital role for enhanced NRFCs structure.

In this study, the Tensile, flexural, and compressive strength of a new set of hybrid composites prepared from Sisal, Nacha, and glass fiber with polyester polymer matrix were characterized based on fiber weight ratio (%wt). To determine the optimal set of composite, the experiment was designed based on Taguchi L_{16} orthogonal array. ANOVA was carried out to determine the contributions of factors that affect the experimental responses. Finally, the multi-linear regression model was developed to determine the error between the experimental and predicted value. The result shows that in the main effect, it was confirmed that Nacha fiber (% wt of N) significantly contributes to tensile, and compressive strength at a 95% level of confidence. Despite the flexural test, neither of the factors shows significant contributions (i.e. P-value > 5%). However, using a linear regression model the optimal values are determined for further exploration. Furthermore, the interaction effects of the factors were also investigated and the following conclusions are drawn;

- All the factors (i.e. %wt of G, %wt of N, and %wt of S) show an interaction effect on tensile and compressive strength. Despite the factors showing linear relationships in levels 2 and 3 of flexural strength, Figure 7 (b).

- Among sixteen Taguchi L_{16} orthogonal array experiments based on the S/N ratio, the four most composites presented in Table 13 are shown promising mechanical properties for wind turbine blade design;
- The average percentage error between the experimental and predicted value are -0.18%, 2.17%, and -0.49% for tensile, flexural, and compressive strengths, respectively.

The percentage error of flexural strength is higher, while the developed mathematical model involves minimizing the errors in the mechanical tests. Through these models, future studies can explore further experiments on fatigue and vibration test of the composite, and conduct finite elements and modal analysis of the real wind turbine blades.

Declarations

Author contribution statement

Temesgen Abriham Miliket: Conceived and designed the experiments; Performed the experiments; Analyzed and interpreted the data.

Mesfin Belayneh Ageze: Conceived and designed the experiments; Wrote the paper.

Muluken Temesgen Tigabu: Conceived and designed the experiments; Analyzed and interpreted the data.

Migbar Assefa Zeleke: Contributed reagents, materials, analysis tools or data.

Funding statement

This research did not receive any specific grant from funding agencies in the public, commercial, or not-for-profit sectors.

Data availability statement

Data included in article/supplementary material/referenced in article.

Declaration of interests statement

The authors declare no conflict of interest.

Additional information

No additional information is available for this paper.

References

- [1] L. Mishnaevsky, K. Branner, H.N. Petersen, J. Beauson, M. McGugan, B.F. Sørensen, Materials for wind turbine blades: an overview, *Materials* 10 (11) (2017) 1285.
- [2] L. Thomas, M. Ramachandra, *Advanced materials for wind turbine blade-A Review*, *Mater. Today Proc.* 5 (1) (2018) 2635–2640.
- [3] A. Gherissi, A study of wind turbine blade structure based on cellulose fibers composite material, *Proc. Eng. Technol.–PET* 38 (2018) 80–85.
- [4] H. Park, A study on structural design and analysis of small wind turbine blade with natural fibre (flax) composite, *Adv. Compos. Mater.* 25 (2) (2016) 125–142.
- [5] M. Tarfaoui, O. Shah, M. Nachtane, Design and optimization of composite offshore wind turbine blades, *J. Energy Resour. Technol.* 141 (5) (2019) 51204.
- [6] W. Muzammil, M.M. Rahman, A. Fazlizan, M. Ismail, H. Phang, M. Elias, *Nanotechnology in renewable energy: critical reviews for wind energy*, in: *Nanotechnology: Applications in Energy, Drug and Food*, Springer, 2019, pp. 49–71.
- [7] U.S. Paulsen, H.A. Madsen, J.H. Hattel, I. Baran, P.H. Nielsen, Design optimization of a 5 MW floating offshore vertical-axis wind turbine, *Energy Proc.* 35 (2013) 22–32.
- [8] H. Su, B. Dou, T. Qu, P. Zeng, L. Lei, Experimental investigation of a novel vertical axis wind turbine with pitching and self-starting function, *Energy Convers. Manag.* 217 (2020) 113012.
- [9] Y. Li, K. Tagawa, W. Liu, Performance effects of attachment on blade on a straight-bladed vertical axis wind turbine, *Curr. Appl. Phys.* 10 (2) (2010) S335–S338.
- [10] D.K. Rajak, D.D. Pagar, P.L. Menezes, E. Linul, Fiber-reinforced polymer composites: manufacturing, properties, and applications, *Polymers* 11 (10) (2019) 1667.

- [11] Y. Golfman, Hybrid Anisotropic Materials for Wind Power Turbine Blades, CRC Press, 2012.
- [12] L. Nguyen, M. Metzger, Optimization of a vertical axis wind turbine for application in an urban/suburban area, *J. Renew. Sustain. Energy* 9 (4) (2017) 43302.
- [13] H. Albers, S. Greiner, H. Seifert, U. Kühne, Recycling of wind turbine rotor blades. Fact or fiction?, in: *Recycling von Rotorblättern aus Windenergieanlagen. Fakt oder Fiktion?* DEWI-Magazin, 2009.
- [14] P. Liu, C.Y. Barlow, Wind turbine blade waste in 2050, *Waste Manag.* 62 (2017) 229–240.
- [15] J.R. Dufloy, Y. Deng, K. Van Acker, W. Dewulf, Do fiber-reinforced polymer composites provide environmentally benign alternatives? A life-cycle-assessment-based study, *MRS Bull.* 37 (4) (2012) 374–382.
- [16] K. Kalkanis, C. Psomopoulos, S. Kaminaris, G. Ioannidis, P. Pachos, Wind turbine blade composite materials-End of life treatment methods, *Energy Proc.* 157 (2019) 1136–1143.
- [17] C.S. Psomopoulos, K. Kalkanis, S. Kaminaris, G.C. Ioannidis, P. Pachos, A review of the potential for the recovery of wind turbine blade waste materials, *Recycling* 4 (1) (2019) 7.
- [18] V. Kouloumpis, R.A. Sobolewski, X. Yan, Performance and life cycle assessment of a small scale vertical axis wind turbine, *J. Clean. Prod.* 247 (2020) 119520.
- [19] N. Suardana, Y. Piao, J.K. Lim, Mechanical properties of hemp fibers and hemp/pp composites: effects of chemical surface treatment, *Mater. Phys. Mech.* 11 (1) (2011) 1–8.
- [20] P. Wambua, J. Ivens, I. Verpoet, Natural fibres: can they replace glass in fibre reinforced plastics? *Compos. Sci. Technol.* 63 (9) (2003) 1259–1264.
- [21] R. Sinha, P. Acharya, P. Freere, R. Sharma, P. Ghimire, L. Mishnaevsky Jr., Selection of Nepalese timber for small wind turbine blade construction, *Wind Eng.* 34 (3) (2010) 263–276.
- [22] L. Mishnaevsky Jr., et al., Strength and reliability of wood for the components of low-cost wind turbines: computational and experimental analysis and applications, *Wind Eng.* 33 (2) (2009) 183–196.
- [23] H. Piggott, *A Wind Turbine Recipe Book: the Axial Flux Windmill Plans*, Scoraig Wind Electric, 2014.
- [24] H. Piggot, "A Wind Turbine Recipe Ebook—The Axial Flux Plans—Metric," Hugh Piggott, Scoraig Wind Electric, Dundonnell, UK, 2014.
- [25] A. Pradeep, S.S. Prasad, L. Suryam, P.P. Kumari, A comprehensive review on contemporary materials used for blades of wind turbine, *Mater. Today Proc.* 19 (2019) 556–559.
- [26] R. Lark, *Fabrication of low cost mod-OA wood composite wind turbine blades*, in: National Aeronautics and Space Administration, Lewis Research Center, 1983.
- [27] K. Jackson, M.v. Zuteck, C. Van Dam, K. Standish, D. Berry, Innovative design approaches for large wind turbine blades, *Wind Energy: Int. J. Prog. Appl. Wind Power Convers. Technol.* 8 (2) (2005) 141–171.
- [28] R.Z. Poore, Advanced blade manufacturing project-final report, in: Sandia National Labs, Sandia National Labs, Albuquerque, NM (US), 1999.
- [29] J.W. Holmes, P. Brøndsted, B.F. Sørensen, Z. Jiang, Z. Sun, X. Chen, Development of a bamboo-based composite as a sustainable green material for wind turbine blades, *Wind Eng.* 33 (2) (2009) 197–210.
- [30] D.U. Shah, P.J. Schubel, M.J. Clifford, Can flax replace E-glass in structural composites? A small wind turbine blade case study, *Compos. B Eng.* 52 (2013) 172–181.
- [31] B. Bakri, S. Chandrabakty, R. Alfriansyah, Potential coir fibre composite for small wind turbine blade application, *Int. J. Smart Mater. Mechatr.* 2 (2015) 42–44.
- [32] S.C. Bakri, et al., Potential coir fibre composite for small wind turbine blade application, *Int. J. Smart Mater. Mechatr.* 2 (2015) 42–44.
- [33] R. Rana, S. Rana, R. Purohit, Characterization of properties of epoxy sisal/glass fiber reinforced hybrid composite, *Mater. Today Proc.* 4 (4) (2017) 5445–5451.
- [34] K. Autar, *Kaw "Mechanics of Composite Materials"* Taylor & Francis Group, LLC, 2006.
- [35] A. Abiy, *Design and Analysis of Bamboo and E-Glass Fiber Reinforced Epoxy Hybrid Composite for Wind Turbine Blade Shell*, Addis Ababa University, 2013.
- [36] H. Bitew, H. Gebregergs, K.B. Tuem, M.Y. Yeshak, Ethiopian medicinal plants traditionally used for wound treatment: a systematic review, *Ethiop. J. Health Dev.* 33 (2) (2019).
- [37] M.S. Hussien, S.T. Desisa, Extraction and Characterization of Ethiopian Hibiscus *Macranthus Bast Fiber*, Extraction, 2019.
- [38] N.R. Council, Assessment of Research Needs for Wind Turbine Rotor Materials Technology, National Academies Press, 1991.
- [39] T. Sathishkumar, P. Navaneethakrishnan, S. Shankar, Tensile and flexural properties of snake grass natural fiber reinforced isophthalic polyester composites, *Compos. Sci. Technol.* 72 (10) (2012) 1183–1190.
- [40] M. Jenberie, Studies on the Mechanical Property Analysis of Bolted Joints of Kusha and Nacha Fiber Composite Laminates, 2020.
- [41] I. Lokantara, N. Suardana, I. Surata, I. Winaya, A review ON natural fibers: extraction process and properties OF grass fibers, *Int. J. Mech. Eng. Technol.* 1 (11) (2020) 84–91.
- [42] G. Gebino, N. Muhammed, Extraction and characterization of Ethiopian pineapple leaf fiber, *Curr. Trend. Fash. Technol. Textile Eng.* 4 (4) (2018) 77–83.
- [43] I.D. Ibrahim, T. Jamiru, E.R. Sadiku, W.K. Kupolati, S.C. Agwuncha, G. Ekundayo, Mechanical properties of sisal fibre-reinforced polymer composites: a review, *Compos. Interfac.* 23 (1) (2016) 15–36.
- [44] E. Bisanda, The effect of alkali treatment on the adhesion characteristics of sisal fibres, *Appl. Compos. Mater.* 7 (5-6) (2000) 331–339.
- [45] S. Chaitanya, I. Singh, Sisal fiber-reinforced green composites: effect of ecofriendly fiber treatment, *Polym. Compos.* 39 (12) (2018) 4310–4321.
- [46] S. Chaitanya, I. Singh, Novel Aloe Vera fiber reinforced biodegradable composites—development and characterization, *J. Reinforc. Plast. Compos.* 35 (19) (2016) 1411–1423.
- [47] M. Cai, H. Takagi, A.N. Nakagaito, Y. Li, G.I. Waterhouse, Effect of alkali treatment on interfacial bonding in abaca fiber-reinforced composites, *Compos. Appl. Sci. Manuf.* 90 (2016) 589–597.
- [48] K.N. Okeke, S.C. Onwubu, G.C. Iwueke, I.O. Arukalam, Characterization of hibiscus sabdariffa fiber as potential reinforcement for denture acrylic resins, *Materia* 23 (2018).
- [49] Y.G. Thyavihalli Girijappa, S. Mavinkere Rangappa, J. Parameswaranpillai, S. Siengchin, Natural fibers as sustainable and renewable resource for development of eco-friendly composites: a comprehensive review, *Front. Mater.* 6 (2019) 226.
- [50] C.C.d. Silva, R.C.S. Freire, E.T.L.C. Ford, C.M. Dantas, J.K. D.d. Santos, E.M. F.d. Aquino, Mechanical behavior and water absorption in sisal/glass hybrid composites, *Materia* 23 (2018).
- [51] R. Payal, Reliable natural-fibre augmented biodegraded polymer composites, in: *Sustainable Polymer Composites and Nanocomposites*, Springer, 2019, pp. 961–975.
- [52] A.A. Betelie, A.N. Sinclair, M. Kortschot, Y. Li, D.T. Redda, Mechanical properties of sisal-epoxy composites as functions of fiber-to-epoxy ratio, *AIMS Mater. Sci.* 6 (6) (2019) 985.
- [53] M. Gupta, R. Srivastava, Properties of Sisal Fibre Reinforced Epoxy Composite, 2016.
- [54] G.R. Kalagi, R. Patil, N. Nayak, Experimental study on mechanical properties of natural fiber reinforced polymer composite materials for wind turbine blades, *Mater. Today Proc.* 5 (1) (2018) 2588–2596.
- [55] A.M. Astm, "ASTM D3039-Standard Test Method for Tensile Properties of Polymer Matrix Composite Materials," Book ASTM D3039-standard test method for tensile properties of polymer matrix composite materials, ASTM International, 2017, p. 2017.
- [56] I. Astm, Standard Test Methods for Flexural Properties of Unreinforced and Reinforced Plastics and Electrical Insulating Materials, 2007. *ASTM D790-07*.
- [57] R.A. Kumar, et al., Wear performance and mechanical properties of unidirectional sisal/carbon/flax hybrid reinforced epoxy composites," in *IOP conference series: materials science and engineering* 988, IOP Publishing, 2020, p. 12010, 1.
- [58] S.C. Tan, Analysis of ASTM D 3410 Compression test specimens, *AIAA J.* 29 (8) (1991) 1344–1346.
- [59] P.R. Lima, R.D. Toledo Filho, J.A. Melo Filho, Compressive stress-strain behaviour of cement mortar-composites reinforced with short sisal fibre, *Mater. Res.* 17 (2014) 38–46.
- [60] O.T. Thomsen, Sandwich materials for wind turbine blades—present and future, *J. Sandw. Struct. Mater.* 11 (1) (2009) 7–26.